Single-Molecule Three-Color FRET

Sungchul Hohng, Chirlmin Joo, and Taekjip Ha
Physics Department, University of Illinois, Urbana-Champaign, Urbana, Illinois

ABSTRACT Fluorescence resonance energy transfer (FRET) measured at the single-molecule level can reveal conformational changes of biomolecules and intermolecular interactions in physiologically relevant conditions. Thus far single-molecule FRET has been measured only between two fluorophores. However, for many complex systems, the ability to observe changes in more than one distance is desired and FRET measured between three spectrally distinct fluorophores can provide a more complete picture. We have extended the single-molecule FRET technique to three colors, using the DNA four-way (Holliday) junction as a model system that undergoes two-state conformational fluctuations. By labeling three arms of the junction with Cy3 (donor), Cy5 (acceptor 1), and Cy5.5 (acceptor 2), distance changes between the donor and acceptor 1, and between the donor and acceptor 2, can be measured simultaneously. Thus we are able to show that the acceptor 1 arm moves away from the donor arm at the same time as the acceptor 2 arm approaches the donor arm, and vice versa, marking the first example of observing correlated movements of two different segments of a single molecule. Our data further suggest that Holliday junction does not spend measurable time with any of the helices unstacked, and that the parallel conformations are not populated to a detectable degree.

INTRODUCTION

Single-molecule fluorescence resonance energy transfer (FRET) between a single donor fluorophore and a single acceptor fluorophore (Ha et al., 1996) has been widely used to study conformational changes of biological molecules and intermolecular interactions (Weiss, 1999, 2000; Ha, 2001, 2004). Time-dependent distance changes between two points labeled with the donor and the acceptor can be traced by recording the time trajectory of FRET efficiency between two fluorophores. For complex molecular dynamics or multicomponents binding interactions, it can be beneficial to have more than one FRET pair to observe correlated changes. An example involving three points is shown in Fig. 1. Using a single pair of fluorophores attached to points 1 and 2, we can determine how close the two points are but there is no information about where the third point is. However, if another dye is attached to point 3 and three distances are obtained, we can determine the relative locations of all three points.

Despite the obvious advantages of three-color FRET over the regular two-color FRET technique, its realization has been hindered by contradictory requirements: a clear spectral separation of three fluorophores' signals and an appreciable amount of FRET between them. For a clear signal separation, the spectral overlap should be small, but this leads to weaker FRET. Several recent studies demonstrated three-color FRET at the ensemble level (Horsey et al., 2000; Ramirez-Carrozzi and Kerppola, 2001; Liu and Lu, 2002; Watrob et al., 2003; Haustein et al., 2003). We have extended three-color FRET to the single-molecule level and measured FRET between one donor and two alternative acceptors to observe correlated movements of different helical arms of a DNA four-way (Holliday) junction undergoing conformational changes.

MATERIALS AND METHODS

Fluorophore selection

FRET between donor and acceptor fluorophores is widely used to examine the conformational properties of biological molecules to which they are attached (Selvin, 2000). The energy transfer efficiency, E, is related to the characteristic Förster distance, R_0, and the distance, R, between the two fluorophores by $E = 1/\{1+(R/R_0)^6\}$. R_0 is defined by Clegg (1992) as

$$R_0 = \left[\frac{9(\ln 10)\Phi^{\mathrm{D}}\kappa^2 \mathrm{j}(\upsilon)}{128\pi^5 \mathrm{N_A} \mathrm{n}^4}\right]^{1/6},$$

where Φ^{D} is the quantum yield of the donor, $J(\nu)$ is the spectral overlap between the donor's emission and the acceptor's absorption, $\mathrm{N_a}$ is Avogadro's number, n is the index of refraction of the medium, and κ is determined by the relative orientation of the two dipole moments.

Ideal fluorophores for single-pair FRET would possess well-separated emission spectra, appreciable overlap between donor emission and acceptor absorption, similar quantum yields of the two fluorophores (for clearly anticorrelated donor and acceptor signal fluctuations that are easily identifiable without any correction), and good photostability. Three-color FRET may require additional criteria for the fluorophore selection depending on particular applications, and can be classified into the following categories according to the spectral separation between three fluorophores: 1) two-donor/one-acceptor scheme; 2) two-step FRET scheme; and 3) one-donor/two-acceptor scheme. These categories are neither exhaustive nor mutually exclusive, and may have pros or cons for specific applications. In the first scheme, the peak emission wavelengths of the two alternate donors are closer to each other than to that of the acceptor. Thus, a single wavelength light source can excite both donors which will be selectively quenched in proportion to the proximity to the acceptor (Ramirez-Carrozzi and Kerppola, 2001). In the two-step FRET scheme, emission peaks of three fluorophores are evenly spaced so that the middle-energy fluorophore acts as a bridge to transfer the excitation from the high-energy to low-energy

Submitted April 1, 2004, and accepted for publication May 17, 2004.

Address reprint requests to Taekjip Ha, E-mail: tjha@uiuc.edu.

0006-3495/04/08/1328/10 $2.00

doi: 10.1529/biophysj.104.043935

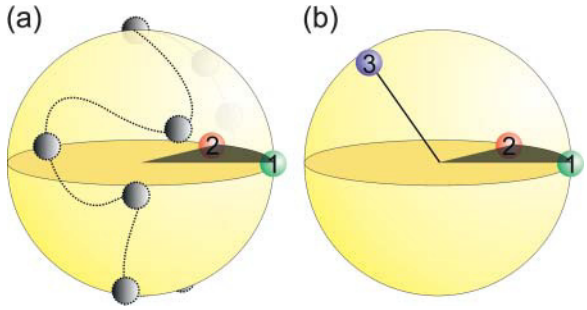

FIGURE 1 A need for three-color FRET. (*a*) A FRET pair attached to the points 1 and 2 reports on the distance between 1 and 2 but no information can be obtained on the position of the point 3. (*b*) By attaching another spectrally distinguishable fluorophore to the point 3 which has appreciable FRET with fluorophores 1 and 2, we can deduce the location of point 3.

fluorophores (Haustein et al., 2003; Watrob et al., 2003). In the one-donor/two-acceptor scheme (Horsey et al., 2000; Watrob et al., 2003), emission peaks of the two acceptors are closer to each other than to the emission peak of the donor, so that the donor might be selectively quenched by either of the acceptor dyes. In this work, we focus on the third scheme.

Cy3 (donor), Cy5 (acceptor 1), and Cy5.5 (acceptor 2) are a good trio for the following reasons. Since Cy5 and Cy5.5 are separated by only 24 nm in the emission peak wavelengths (670 nm and 694 nm, respectively) and share similar extinction coefficients (250,000 M^{-1} cm^{-1} for both of them, according to Amersham Biosciences, Piscataway, NJ), the spectral overlap integral (Clegg, 1992) for the Cy3-Cy5.5 pair is only slightly lower, a factor of 0.88, than that of the Cy3-Cy5 pair. The spectral overlap integral for the Cy5-Cy5.5 pair is substantially larger, being 3.31-times that of the Cy3-Cy5 pair. Using measured values of quantum yields of DNA-conjugated Cy3 and Cy5 (Murphy et al., 2004) and assuming the orientational factor κ^2 is 2/3, Förster distances (R_0 values) were calculated to be 6.0 nm, 5.9 nm, and 7.3 nm for the Cy3-Cy5, Cy3-Cy5.5, and Cy5-Cy5.5 pairs respectively. This choice of fluorophores causes similar levels of FRET from the donor to either of the acceptors for a given distance, and is therefore ideal in determining which of the two alternative acceptors are closer to the donor. The distance between Cy5 and Cy5.5 remains large for our model system of Holliday junction such that FRET between them is relatively small despite the large R_0.

Optics for three-color FRET and bleedthrough correction scheme

Because of the large spectral overlap between Cy5 and Cy5.5, a judicious selection of optimal dichroic mirrors and bandpass filters was crucial for clearly separating signals arising from three fluorophores. All optics mentioned below were purchased from Chroma Technology (Brattleboro, VT). Nominal cutoff wavelengths of dichroic mirrors were 650 nm (650 drxr, extra reflection region, longpass) for separating Cy3 emission from others, and 690 nm (690dclp, longpass) for further separating fluorescence signals from Cy5 and Cy5.5. To reduce bleedthrough between detection channels, additional bandpass filters were used (HQ580/60 m, 60-nm transmission window centered at 580 nm, for Cy3 channel, HQ670/40 m for Cy5 channel, and HQ715/30 m for Cy5.5 channel). The cutoff wavelength of a dichroic mirror is a sensitive function of the incident angle. We intentionally made the incident angle to 690dclp ~50° instead of 45° to minimize Cy5.5 signal bleedthrough to Cy5 channel. Therefore, the true cutoff wavelength is ~685 nm. As can be deduced from Fig. 2 *a*, bleedthrough of Cy5 and Cy5.5 emission to Cy3 channel is negligible. However, there is significant amount of bleedthrough of the Cy5 emission into the Cy5.5 channel and of the Cy5.5 emission into the Cy5 channel. Also a small but measurable amount of Cy3 emission appears in both the Cy5 and Cy5.5 channels.

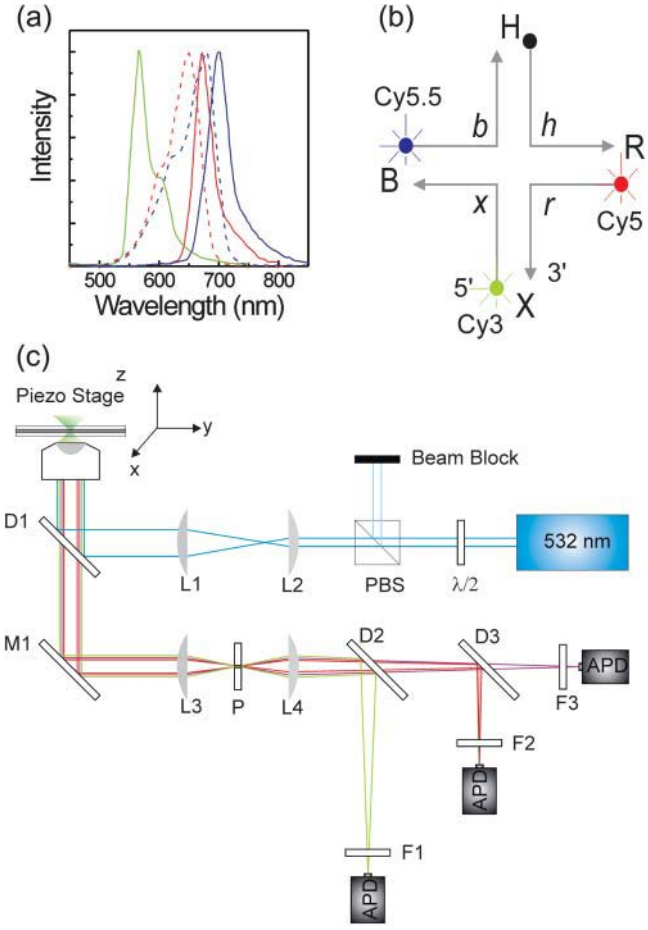

FIGURE 2 (*a*) Normalized emission (*solid lines*) and absorption spectra (*dashed lines*) of Cy3 (*green*), Cy5 (*red*), and Cy5.5 (*dark blue*). (*b*) Schematics of the Holliday junction. The Holliday junction is a four-way DNA junction composed of four helical arms (marked *X*, *R*, *H*, and *B*). The polarity of the comprising strands (*x*, *r*, *b*, and *h*) is indicated by the arrowheads (5′–3′). We abbreviate the dye configuration of each vector by denoting helix names superscripted by dye tagged to it. In the figure, Holliday junction is labeled with Cy3 (*green*) on helix *X*, Cy5 (*red*) on helix *R*, and Cy5.5 (*dark blue*) on helix *B*. Using this convention, it is named $X^3R^5B^{5.5}$. (*c*) Schematic setup of the single-molecule three-color FRET experiments. The confocal setup was made on an inverted microscope (Olympus, IX50). A solid-state laser (CrystaLaser) excites a sample at 532-nm through a 100× oil-immersion objective. Emission from three dyes is collected by the same objective and separated by dichroic mirrors and filtered out by bandpass filters. Identities of symbols are *D1*, Chroma dichroic 545drlp; *D2*, Chroma dichroic 650 drxr; *D3*, Chroma dichroic 690dclp; *F1*, Chroma filter HQ580/60 m; *F2*, Chroma filter HQ670/40 m; *F3*, Chroma filter HQ715/30 m; *M*, mirror; *L*, lens; *P*, pinhole; *PBS*, polarizing beam splitter; λ/2, half-waveplate; and *APD*, avalanche photo diode.

Our model for bleedthrough correction and experimental values of bleedthrough parameters are summarized in Table 1. The identities of symbols are

I_3, total signal of Cy3.
I_5, total signal of Cy5.
$I_{5.5}$, total signal of Cy5.5.
A'', total signal detected by Cy3 channel.
B'', total signal detected by Cy5 channel.

TABLE 1 Bleedthrough estimation

	Ch1 (A'')	Ch2 (B'')	Ch3 (C'')
Cy3 (I_3)	A	$\alpha \times A$ ($\alpha = 0.05$)	$\beta \times A$ ($\beta = 0.04$)
Cy5 (I_5)	0	B	$\gamma \times B$ ($\gamma = 0.96$)
Cy5.5 ($I_{5.5}$)	0	$\delta \times C$ ($\delta = 0.15$)	C

The identities of symbols used are: I_3, total signal of Cy3; I_5, total signal of Cy5; $I_{5.5}$, total signal of Cy5.5; A'', total signal detected by Cy3 channel; B'', total signal detected by Cy5 channel; C'' total signal detected by Cy5.5 channel; A, Cy3 signal detected in Cy3 channel; B, Cy5 signal detected in Cy5 channel; C, Cy5.5 signal detected in Cy5.5 channel; and α, β, γ, and δ are bleedthrough parameters. As an example, α denotes the amount of Cy3 signal detected in Cy5 channel in units of A. We assume no bleedthrough of Cy5 and Cy5.5 3 emission into the Cy3 channel. Numbers in the parentheses were obtained as explained in the caption of Fig. 4.

C'', total signal detected by Cy5.5 channel.
A, Cy3 signal detected in Cy3 channel.
B, Cy5 signal detected in Cy5 channel.
C, Cy5.5 signal detected in Cy5.5 channel.
α, β, γ, and δ are bleedthrough parameters as described in Table 1.

We assume no bleedthrough of Cy5 and Cy5.5 emission into Cy3 channel. Therefore,

$$A'' = A, \tag{1}$$

$$B'' = \alpha \times A + B + \delta \times C, \tag{2}$$

$$C'' = \beta \times A + \gamma \times B + C. \tag{3}$$

From the measured quantities of A'', B'', C'', α, β, γ, and δ, the fluorescence signals of the three dyes (I_3, I_5, and $I_{5.5}$) after bleedthrough a correction can be calculated as follows:

1. Subtract bleedthough of Cy3 signal from Eqs. 2 and 3.

$$B' = B'' - \alpha \times A = B + \delta \times C, \tag{4}$$

$$C' = C'' - \beta \times A = \gamma \times B + C. \tag{5}$$

2. Calculate B and C by solving linear Eqs. 4 and 5.

$$B = (B' - \delta \times C')/(1 - \gamma \times \delta), \tag{6}$$

$$C = (C' - \gamma \times B')/(1 - \gamma \times \delta). \tag{7}$$

3. Calculate I_3, I_5, $I_{5.5}$ by adding back bleedthrough to other channels.

$$I_3 = (1 + \alpha + \beta) \times A, \tag{8}$$

$$I_5 = (1 + \gamma) \times B, \tag{9}$$

$$I_{5.5} = (1 + \delta) \times C. \tag{10}$$

4. Calculate apparent FRET efficiencies to Cy5 and Cy5.5.

$$E_5 = I_5/(I_3 + I_5 + I_{5.5}),$$

$$E_{5.5} = I_{5.5}/(I_3 + I_5 + I_{5.5}).$$

DNA preparation

Oligonucleotides of the following sequences (all written 5′ to 3′) were purchased from IDTDNA:

x strand: CCCAGTTGAGAGCTTGCTAGGG (unlabeled or 5′-Cy3),
b strand: CCCTAGCAAGCCGCTGCTACGG (unlabeled or 5′-Cy5.5),
r strand: CCCACCGCTCTTCTCAACTGGG (unlabeled, 5′-Cy5 or 5′-biotin),
h strand: CCGTAGCAGCGAGAGCGGTGGG (5′-Cy5 or 5′-biotin).

The appropriate four strands required to generate a particular labeling configuration were annealed by heating the strands to 90°C in 10 mM Tris (pH 8.0), 50 mM of NaCl, followed by slow cooling to room temperature. The ratio of the concentration of the four strands was 1:1:1:1, with a final concentration of ~5 μM in the total volume of ~90 μl. Each vector is named by writing the helical arms superscripted by a number denoting the fluorophore attached. The unmentioned arm or the arm H, when more than two arms are not mentioned, is labeled with biotin. For example, $X^3R^5B^{5.5}$ depicted in Fig. 2 *b* has Cy3 (*green*) on arm X, Cy5 (*red*) on arm R, Cy5.5 (*dark blue*) on arm B, and biotin (*black*) on arm H.

Single-molecule fluorescence measurements

For single-molecule experiments, a narrow channel was made between a cleaned microscope slide and a coverslip using double-sided adhesive tape. Holliday junctions were attached to the surface by successive additions of 40 μl of 1 mg/ml biotinylated BSA (Sigma, St. Louis, MO), 40 μl of 0.2 mg/ml streptavidin (Molecular Probes, Eugene, OR), and 40 μl of 10–50 pM biotinylated Holliday junction in 10 mM Tris:HCl (pH 7.5), 50 mM NaCl (TN buffer). Each addition was incubated for 10 min, and followed by washing with TN buffer. The concentration of the DNA solution was adjusted to give a good surface density for the single-molecule experiments. After checking that fluorescent spots were well separated from one another, we injected 60 μl of the imaging buffer (10 mM Tris:HCl, pH 7.5 and 50 mM Mg^{2+} if not mentioned otherwise) containing 0.4% (w/v) glucose, 1% (v/v) 2-mercaptoethanol, 0.1 mg/ml glucose oxidase (Sigma), and 0.02 mg/ml catalase (Roche, Nutley, NJ). Schematics of the experimental setup are drawn in Fig. 2 *c*. The confocal microscope is based on an inverted microscope (Olympus IX50) with a 100× oil immersion objective with numerical aperture of 1.4 (Olympus America, Melville, NY) and three silicon avalanche photodiode photon counting units (PerkinElmer, Wellesley, MA) to record fluorescence intensities from a single molecule under a focused laser spot. A solid-state 532-nm laser (CrystaLaser, Reno, NV) was used to excite the molecules. Data were acquired at room temperature using a program written in Visual C++ (Microsoft, Seattle, WA). Molecules showing all two or three dyes, depending on the configuration, as well as dynamic changes in FRET were chosen for analysis to exclude molecules with inactive fluorophores or missing strand(s).

RESULTS AND DISCUSSIONS

Holliday junction conformational states

The Holliday junction is a key intermediate in homologous DNA recombination, and consists of four strands of DNA joined at a four-way junction. Fig. 3 illustrates the currently accepted model of Holliday junction dynamics (Lilley, 2000). In the presence of metal ions such as magnesium, the Holliday junction folds into the x-shape structure via pairwise coaxial stacking of neighboring helices. There are two ways of stacking four helices (X, B, R, and H) in pairs. In one of the stacking conformers, helix X is stacked on helix B and helix H is stacked on helix R. In the other stacking

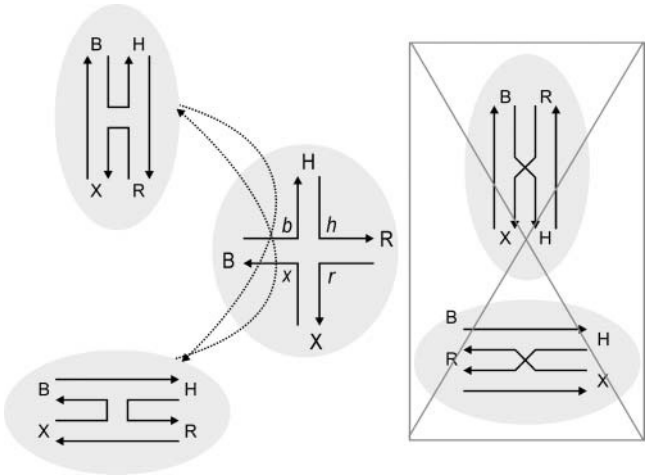

FIGURE 3 Conformational states of Holliday junction. In the presence of metal ions, Holliday junctions fold by coaxial stacking of helical arms in pairs; adjacent helices become straight. Two possibilities of stacking are *B*-on-*X* (thus *H*-on-*R*) and *X*-on-*R* (thus *B*-on-*H*). Component strands can be divided into two classes. Continuous strands have a single axis, whereas exchanging strands pass between axes at the junction point. In extreme cases, each stacking conformer can be distinguished further depending on relative orientation of two stacked helices. In antiparallel forms, the polarity of the continuous strands run in opposite directions, whereas in parallel forms they have the same direction. In reality, the junction can have any angle between the parallel and antiparallel forms. The Holliday junction is known to continuously switch between two antiparallel conformers through the open state. No parallel state has been observed experimentally.

conformer, helix *X* is stacked on helix *R* and helix *H* on helix *B*. According to the relative orientations of DNA strands, each stacking conformer can be further classified as parallel or antiparallel. In the antiparallel forms, the polarity of the continuous strands runs in opposite directions, whereas in the parallel forms they have the same direction. Various structural studies have detected only the antiparallel forms (Duckett et al., 1988; Murchie et al., 1989; Nowakowski et al., 1999; Ortiz-Lombardia et al., 1999; Eichman et al., 2000) and no evidence for parallel forms exists yet. The relative stability of each stacking conformer depends on the local sequence immediately surrounding the junction. The junction used for our studies is known to favor the *X*-on-*R* stacking over the *X*-on-*B* stacking (Duckett et al., 1988). A continuous exchange between the two stacking conformers was observed via single-molecule FRET measurements and was shown to slow down with increasing Mg^{2+} ion concentration with no change in the relative population of the two conformers (McKinney et al., 2003). The conformer bias observed in single-molecule measurements matched the bias observed in bulk solution gel electrophoresis studies on unlabeled junctions. In addition, moving the fluorophores and biotin to different arms did not alter the conformer transition rates (Joo et al., 2004). Therefore the effects of dye labeling and surface immobilization were not significant in two-color single-molecule FRET studies. These previous studies, however, could not tell if the movements of the four arms are simultaneous or some segments can move independently of others. For instance, does helix *B* approach helix *X* as helix *R* simultaneously moves away from helix *X*? These types of questions cannot be addressed using only two fluorophores. Below, we show data obtained using two fluorophores (Cy3-Cy5 or Cy3-Cy5.5), one donor and two identical acceptors (Cy3-Cy5-Cy5), and one donor and two different acceptors (Cy3-Cy5-Cy5.5).

Holliday junction dynamics probed by one donor and two identical acceptors

In this section, we measured the $X^3R^5B^5$ vector, which is shorthand for a labeling scheme where Cy3 is on helix *X* and the Cy5's are on helix *R* and helix *B* (see Materials and Methods for naming convention), using a two-color setup for Cy3 and Cy5 signals. In one stacking conformer, the helix *R* is close to the helix *X* that carries the donor (Cy3), whereas in the other conformer, it is the helix *B* that is close to the helix *X*. Since both helix *R* and helix *B* carry one acceptor (Cy5) each, we expect to see a constant level of FRET provided that 1), there is no other conformation populated and that 2), the distance between the donor and the acceptor on helix *R* in the *X*-on-*B* conformer is identical to the distance between the donor and the acceptor on helix *B* in the *X*-on-*R* conformer.

As Fig. 4, *a* and *b*, show, FRET signals remain constant when both acceptors are active except for brief excursions to lower FRET values. These apparent FRET values were calculated as the ratio between the signal in acceptor channel and the total signal detected by both channels. Experiments were performed with 30 mM Mg^{2+} and 50 mM Na^{+}. After the photobleaching of one of the acceptors, marked by a dotted vertical line, fluorescence signals are due solely to X^3B^5 or X^3R^5 and favor high or low FRET states respectively, depending on which acceptor bleaches first. This result suggests that the junction structures are symmetric enough between the two conformers so that the two alternative acceptors share similar distances to the donor when each is brought close to the donor. However, the observation of short-lived low FRET states here with 8-ms time resolution cannot be interpreted unambiguously. They can be due to photophysical properties of the fluorophores (for example, we have observed occasional blinking of Cy5 in the absence of other dyes) or due to other minority species of the Holliday junction such as parallel or partially stacked structures.

Single Holliday junction dynamics with two-color FRET and bleedthrough estimation

As preparation for three-color FRET measurements, we have performed single-molecule measurements of Holliday junctions labeled with Cy3 and Cy5 (X^3R^5) or with Cy3 and Cy5.5 ($X^3B^{5.5}$). Cy3 and Cy5 were used in previous single-molecule studies of the Holliday junction dynamics

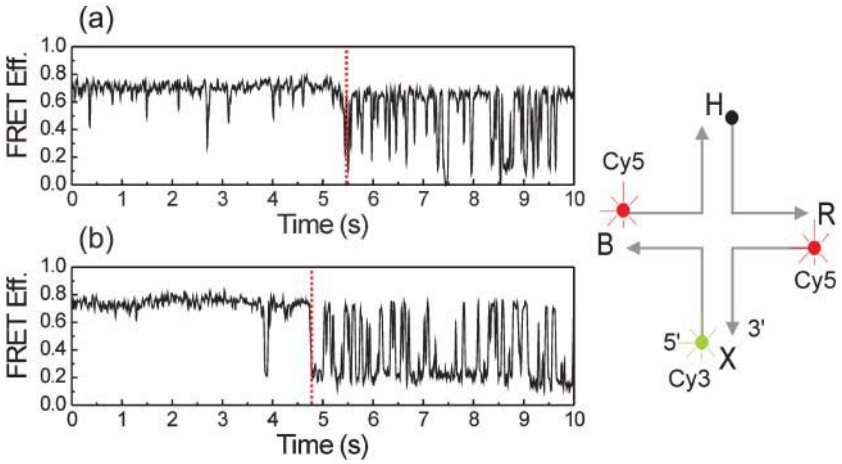

FIGURE 4 Single Holliday junction dynamics using one donor and two identical acceptors. (*a* and *b*). Two-color FRET experiment on $X^3R^5B^5$. When both of the two acceptors are active, the acceptor signals are almost constant, which supports the model depicted in Fig. 3. After one of the two acceptors bleaches (*dotted red lines*), time-traces show kinetics similar to X^3B^5 (*a*) or X^3R^5 (*b*), depending on which acceptor bleaches.

(McKinney et al., 2003) using two-color configuration. The current measurements were performed with three detectors that record Cy3, Cy5, and Cy5.5 channels simultaneously. Time-traces in Fig. 5 *a*, and *b*, show the time records of these three channel signals before any correction for bleedthrough is made. The donor signal primarily shows up in the Cy3 channel whereas the acceptor signals are seen exclusively in the channels for Cy5 and Cy5.5. Clearly anticorrelated fluctuations of respective donor and acceptor signals were observed representing stacking conformer transitions of single Holliday junctions. The transition rates were determined via dwell-time analysis and were nearly identical, regardless of labeling configuration (see below). These rates are also independent of excitation power, but strongly dependent on the DNA sequence and ionic conditions (McKinney et al., 2003), hence they cannot be due to photophysical effects or fluorophore specific artifacts. These data show that the Holliday junction dynamics can be measured reliably using Cy3 and Cy5.5 as a FRET pair.

We also estimated the bleedthrough parameters (α, β, γ, and δ) listed in Table 1 from these control experiments. Cy3 signal bleedthrough to the acceptor channels, α and β, were obtained from signals after acceptor bleaching. From the early part of the data when the acceptor is active, the distribution of acceptor signal between Cy5 and Cy5.5 channels is obtained after correcting for Cy3 bleedthrough. For example, from the initial part of Fig. 5 *a* before Cy5 bleaching, we can obtain γ. In the same way, we get δ from Fig. 5 *b*. All bleedthrough parameters are averaged from ~20 molecules.

Correlated motions of single Holliday junction probed by three-color FRET

To observe correlated conformational changes of the Holliday junction directly, we made the $X^3R^5B^{5.5}$ vector, which is labeled with Cy3 on helix *X*, Cy5 on helix *R*, and Cy5.5 on helix *B*. Fig. 6, α and β, are typical three-color time-traces of I_3, I_5, and $I_{5.5}$ after bleedthrough has been corrected for as discussed in Materials and Methods. All data are collected with 20-ms bin time. Approximately 5% of molecules in our preparation had all three fluorophores active. This low yield

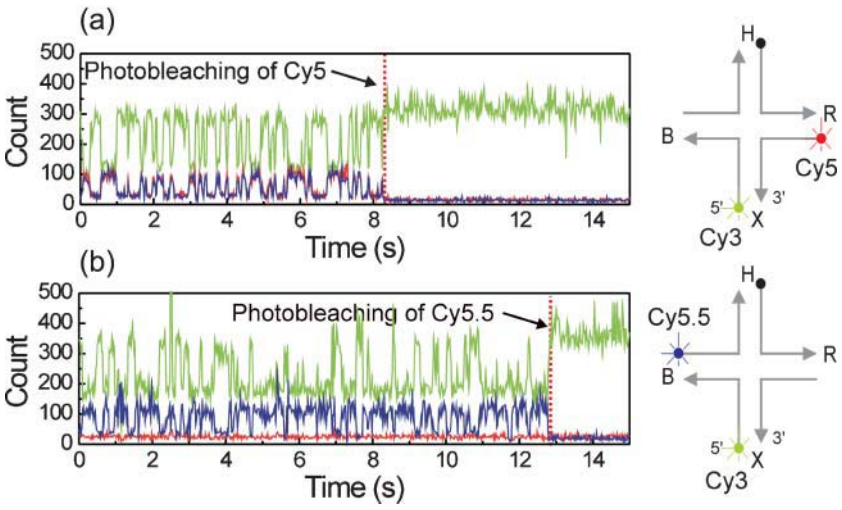

FIGURE 5 Single Holliday junction dynamics using one donor and one acceptor, measured in three-color setup (control experiments for bleedthrough correction). Experiments were performed at room temperature in 10 mM Tris buffer with 50 mM Mg^{2+}. (*a*) Time-traces of the X^3R^5 vector which is tagged with Cy3 on helix *X* and Cy5 on helix *R*. After Cy5 bleaches (*dotted red lines*) the bleedthrough from Cy3 emission into channel 2 (*red lines*) and channel 3 (*dark blue lines*) is estimated to be 5% and 4%, respectively. The distribution of Cy5 signal in channel 2 and channel 3 is 1:0.96 from the initial part of traces after subtracting Cy3 bleedthrough. (*b*) Time-traces of $X^3B^{5.5}$ which is tagged with Cy3 on helix *X* and Cy5.5 on helix *B*. Emission of Cy5.5 is distributed in channel 2 and channel 3 with a ratio of 0.15:1.

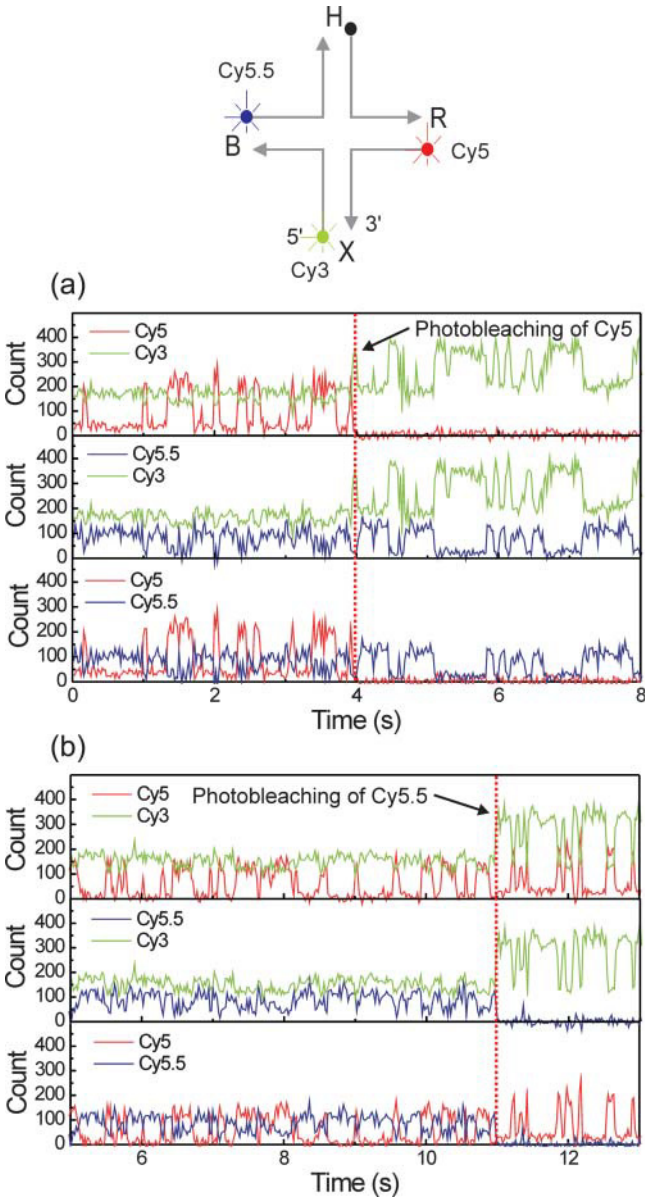

FIGURE 6 Intensity time-traces of $X^3R^5B^{5.5}$. All signals are corrected for bleedthrough. When the three dyes are active, anticorrelation between Cy5 and Cy5.5 signals are clear. After one of the two acceptors photobleaches, time-traces show the behavior of (*a*) $X^3B^{5.5}$ or (*b*) X^3R^5, depending on which acceptor bleaches first.

could be due to inactive acceptor molecules (typically less than half of Cy5 or Cy5.5 molecules are active for two-color FRET experiments) as well as molecules that are not complete since we did not purify four-stranded molecules after junction assembly. For an easier inspection of the data, intensity time-traces of the three dyes (Cy3 in *green*, Cy5 in *red*, and Cy5.5 in *dark blue*) are plotted in pairs in three different graphs.

In Fig. 6 *a*, Cy5 bleaches first at ~4 s (marked by a *dotted red line*) and the behavior of the $X^3B^{5.5}$ vector appears afterward. When Cy5.5 bleaches first as in Fig. 6 *b*, a bias to the low FRET state is observed as in X^3R^5 vector. When all three dyes are active, Cy5 and Cy5.5 signals fluctuate in an anticorrelated manner, which is clear evidence for an unambiguous separation of Cy5 and Cy5.5 signals despite significant bleedthrough between the two channels. The anticorrelated fluctuation of Cy5 and Cy5.5 signals is consistent with the presently accepted model that helix *X* alternatively comes close to helices *R* and *B*. The donor signal fluctuates by a relatively small amount but is slightly more quenched when the Cy5 signal is strong compared to when the Cy5.5 signal is strong. Therefore, the donor is continuously quenched by either of the acceptors, suggesting that movements of helices *B* and *R* to and from helix *X* are well-synchronized. Slightly better quenching of Cy3 by Cy5 than by Cy5.5 may be due to a larger spectral overlap between Cy3 and Cy5 rather than to geometric differences such as distance and orientation because we observed no time-dependent changes of the donor signal when two identical acceptors were used instead (Fig. 4). It is noticeable that the Cy5.5 signal intensity of the high FRET state increases after Cy5 bleaches in Fig. 6 *a* and vice versa in Fig. 6 *b*. Competition between FRET from Cy3 to Cy5 and FRET from Cy3 to Cy5.5 partly explains the difference, but there definitely exist effects of two-step FRET from Cy3 to Cy5 to Cy5.5; Cy5.5 intensity in its low FRET state is higher when Cy5 is active than after Cy5 bleaching (Fig. 6 *a*). The extent of FRET between Cy5 and Cy5.5 will be quantified below.

Dwell-time analysis of doubly and triply labeled Holliday junction

We performed dwell-time analysis for $X^3R^5B^{5.5}$, X^3R^5, and $X^3B^{5.5}$ vectors under the same conditions. The high FRET state for Cy5 of $X^3R^5B^{5.5}$, the high FRET state of X^3R^5, and the low FRET state of $X^3B^{5.5}$ all correspond to the *X*-on-*B* stacked antiparallel state whereas the *X*-on-*R* stacked antiparallel state yields the low FRET state for Cy5 of $X^3R^5B^{5.5}$, the low FRET state of X^3R^5, and the high FRET state of $X^3B^{5.5}$. Fig. 7 shows the dwell-time histograms with single exponential decay fits. The resulting dwell-times are 0.11 s, 0.16 s, and 0.13 s for the *X*-on-*B* stacked state and 0.23 s, 0.35 s, and 0.23 s for the *X*-on-*R* stacked state. Since these times are similar with the relative standard deviation of 19% and 26% respectively, we conclude the effect of dye labeling on the junction dynamics is not significant.

Complete stacking and no parallel states

In a parallel state as illustrated in Fig. 3, the $X^3R^5B^{5.5}$ vector would give low FRET for both Cy5 and Cy5.5 acceptors. If stacking is incomplete, for instance if one pair of helices unstacks significantly earlier than the other pair of helices, the transitions in Cy5 and Cy5.5 signals may not be simultaneous. In these respects, the time-traces in Fig. 6 support the current model of Holliday junction conformations; complete stacking and no parallel state. To elucidate

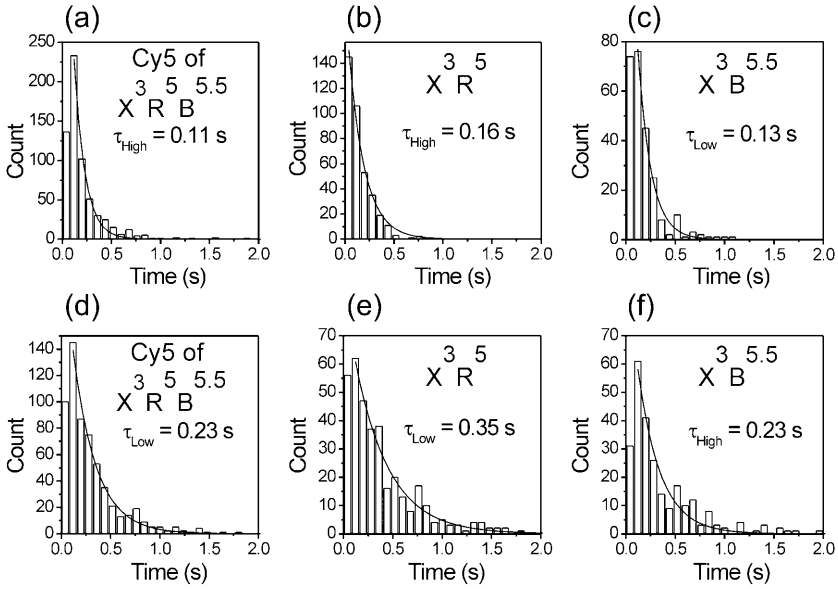

FIGURE 7 Dwell-time analysis of two conformations measured from Holliday junctions. Different labeling configurations are indicated. Single-exponential fits are also shown. The first bin is not included in the fitting procedure to account for missing short dwell-time events.

these matters more quantitatively, we performed additional data analyses as shown in Fig. 8, *a* and *b*.

The two-dimensional histogram of apparent FRET efficiencies of Cy5 (E_5) versus those of Cy5.5 ($E_{5.5}$) shows two well-separated regions (Fig. 8 *a*, obtained from ~60 molecules). Negligible number of data point in the left-bottom region indicates the absence of parallel states. Highly-populated regions are elongated with a negative slope due to bleedthrough correction. Eqs. 6 and 7 have negative terms proportional to C' or B'. Therefore, a noise-induced increase of signal in one channel brings about a decrease in the other channel, leading to an anticorrelated behavior between E_5 and $E_{5.5}$ within each region.

We also tested for the coincidence of Cy5 and Cy5.5 transitions. Transition times were determined using a computer algorithm. In the algorithm used, the apparent FRET

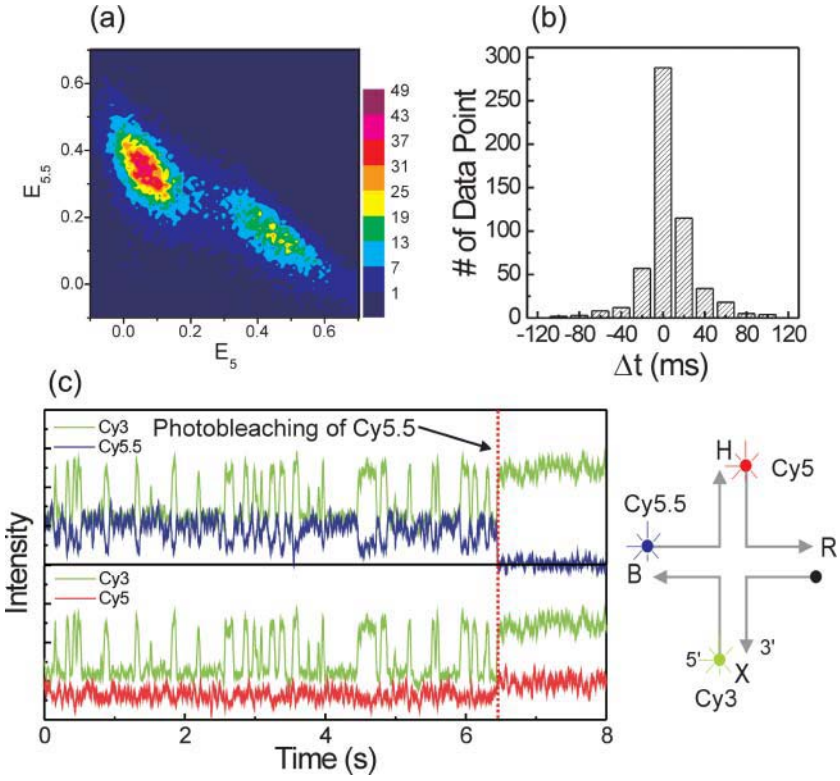

FIGURE 8 Completeness of stacking and no parallel state. (*a*) Relative distribution of apparent Cy5 FRET efficiency (E_5) and apparent Cy5.5 FRET efficiency ($E_{5.5}$). Data were collected from ~60 molecules. (*b*) Histograms of transition time difference between Cy5.5 and Cy5 signals. (*c*) Time-traces of $X^3H^5B^{5.5}$. FRET fluctuation between Cy3 and Cy5.5 is clear and we conclude this is a ''real'' molecule. However, no high FRET state was observed for Cy5 indicating the absence of stable parallel states.

efficiencies were first normalized so that the low FRET state is set to zero and the high FRET state is set to 1. Molecules were considered to be in the low FRET state if the normalized value is <0.3 and in the high FRET state if the normalized value is >0.5. When values are between 0.3 and 0.5, molecules were assigned to the previous state to avoid false identification of fast transitions due to noise. The difference between a Cy5.5 transition event and Cy5 transition event, Δt, was determined by matching recorded conformational transitions in both channels. The result from 20 molecules is summarized in Fig. 8 *b* as a histogram of Δt. 84% of data points fall within the integration time used (20 ms). This, therefore, supports the conclusion that the stacking and unstacking of the two pairs of helices are very well synchronized within 20 ms although noise in the data prevents us from placing a precise limit on the degree of synchrony.

Exploring parallel states using three-color FRET

Perhaps the most direct way to test for the existence of parallel states is to study a junction labeled in such a way that only parallel states would show high FRET, for instance X^3H^5. Indeed, our previous studies of X^3H^5 strongly indicate the lack of parallel states longer than 5 ms (Joo et al., 2004). However, one of the most time-consuming and subjective steps in these studies was to discern a ''real'' molecule, a complete four-way junction with all intended fluorophores, from other contaminants such as incomplete molecules or impurities. This can be a common problem when one tries to detect a very rare event since there is no easy way to tell whether an interesting time record is from a ''real'' molecule or other artifacts. In this respect, having an additional acceptor, for example Cy5.5 attached to the helix *B*, can be very helpful because FRET between Cy3 and Cy5.5 shows whether the molecule is ''real'' whereas FRET between Cy3 and Cy5 can be used to seek parallel states.

Fig. 8 *c* shows fluorescence time records obtained from a $X^3H^5B^{5.5}$ vector in 10 mM Tris:HCl, pH. 7.4, 50 mM Mg^{2+} at 20°C with 6-ms time resolution. Although the anticorrelated fluctuation between Cy3 and Cy5.5 shows that the molecule displays the expected Holliday junction conformational dynamics, there is no high FRET state observed between Cy3 and Cy5—indicating that the parallel state, even if it exists, must be shortlived. We did not observe any parallel state for a total observation time of 147 s from 17 molecules. No parallel states were observed at lower temperature (2°C achieved via Peltier cooling in contact with the sample slide), regardless of the presence of 50 mM NaCl. We conclude that parallel states longer than 6 ms are exceedingly rare.

Estimating true FRET efficiencies and distances

For most applications, we are mainly interested in the kinetic information obtained from qualitatively relating FRET values to distinct conformations. Yet for more complex systems, absolute distance information may become necessary in making such assignments. In the following, we attempt to obtain absolute distances for the *X*-on-*B* antiparallel state based on single-molecule three-color FRET data. In principle, in addition to FRET from Cy5 to Cy5.5, FRET from Cy5.5 to Cy5 is possible due to the large amount of overlap between Cy5.5 emission and Cy5 absorption. However, in the *X*-on-*B* antiparallel state, direct FRET from Cy3 to Cy5.5 is small compared with direct FRET from Cy3 to Cy5 and we can disregard energy flow from Cy5.5 to Cy5. Therefore, their interaction map is simplified as depicted in Fig. 9 *a*. In the figure, dye 1 (*green*), dye 2 (*red*), and dye 3 (*dark blue*) correspond to Cy3, Cy5, and Cy5.5, respectively. Only dye 1 is directly excited by the light source with the rate of G_0. This is a good assumption for this work because absorption of Cy5 and Cy5.5 at 532 nm is less than 1/30th of their peak absorption. We note, however, that correction due to direct excitation of the acceptors could become significant if we were to measure very low FRET. The rate constants k_i ($i = 1, 2, 3$) represents decay rates of i^{th} dye in the absence of FRET and k_{ij} ($i < j$) is fluorescence energy transfer rate from the i^{th} dye to the j^{th} dye.

To estimate the distances between i^{th} and j^{th} dyes (D_{ij}, $i < j$), we need to obtain the three FRET efficiencies, E_{12}, E_{13}, and E_{23}, as would be measured when only two of the dyes are fluorescing. E_{12} and E_{13} are obtained with relative ease by utilizing acceptor photobleaching or blinking. In region II of Fig. 9 *b*, Cy5.5 is not active and only FRET from Cy3 to Cy5 occurs. To calculate E_{12} from Cy3 and Cy5 signals, we need a calibration factor φ which is a measure of how much the Cy3 signal decreases relative to the increase in the Cy5 signal when a conformational change occurs (as has been defined as γ in Ha et al., 1999). From the intensity histograms of Cy3 and Cy5 which are made from the region II, φ is 1.27. E_{12} is expressed as $\varphi \times I_2/(I_1 + \varphi \times I_2)$ (Ha et al., 1999) and we obtain 0.68. In the same way, E_{13} is 0.10 from the region III. Using the previously calculated R_0 values, $D_{12} = 5.3$ nm and $D_{13} = 8.5$ nm.

To deduce E_{23} we can follow the treatment of three-color FRET by Watrob et al. (2003). Let us denote intensities of i^{th} dye when all three dyes are active as I_i ($i = 1$, 2, and 3). They can be expressed as follows after discarding common proportional factors:

$$I_1 = 1/(k_1 + k_{12} + k_{13}), \tag{11}$$

$$I_2 = E^*_{12} \times 1/(k_2 + k_{23}), \tag{12}$$

$$I_3 = (E^*_{12} \times E_{23} + E^*_{13}) \times 1/k_3, \tag{13}$$

where

$$E^*_{12} = k_{12}/(k_1 + k_{12} + k_{13}), \tag{14}$$

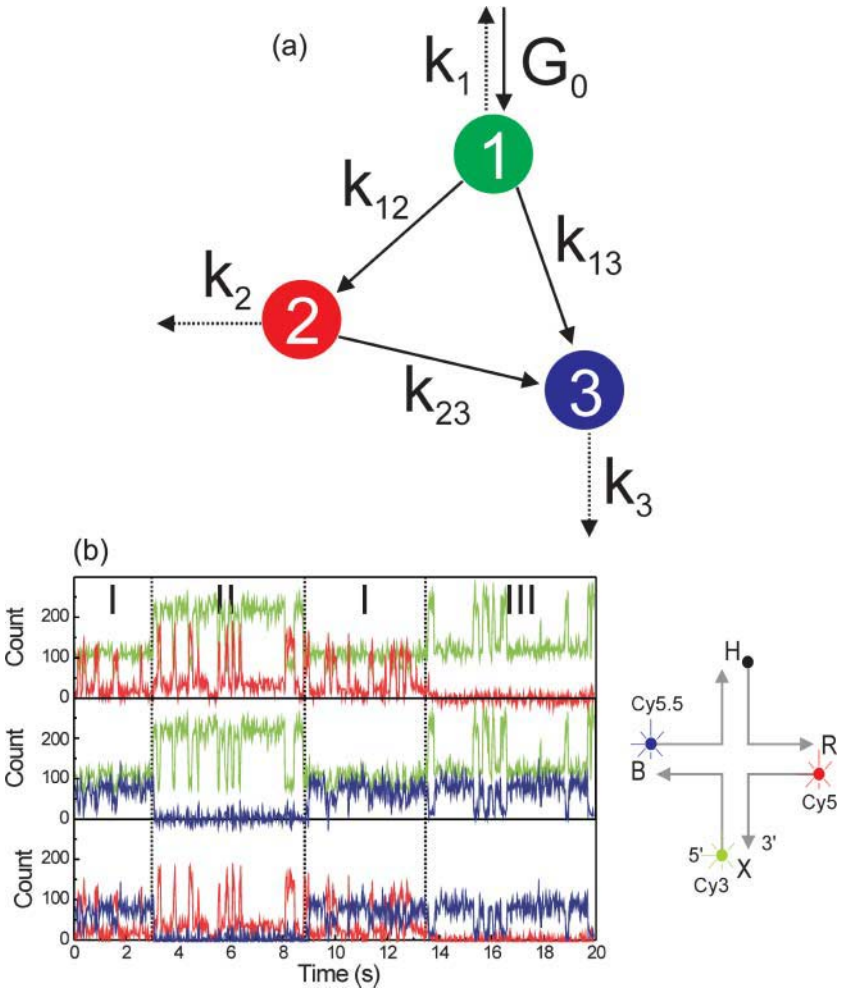

FIGURE 9 Calculation of distances between three dyes. (*a*) Interaction map among three dyes. Dye 1 (*green*), dye 2 (*red*), and dye 3 (*dark blue*) represent high-, middle-, and low-energy dyes, respectively. We assume only dye 1 is excited with the generation rate of G_0. The decay rate k_i (i = 1, 2, and 3) is the sum of radiative and nonradiative decay rates of the i^{th} dye when there is no FRET interaction. The rate k_{ij} represents energy transfer rate from the i^{th} dye to the j^{th} dye. (*b*) Three-color FRET time-traces (Cy3 in *green*, Cy5 in *red*, and Cy5.5 in *dark blue*) which were used to derive distances between three dyes. In the region I, the three dyes are all active. In the region II, Cy5.5 is inactive and data from this region is used for calculating E_{12}. Using data in region III where Cy5 is bleached, E_{13} is calculated. As explained in the text, E_{23} is calculated by comparing Cy5 intensities in regions I and II or in regions I and III. Distances between the three dyes are readily obtained from E_{12}, E_{13}, and E_{23} using the calculated values for R_0 for each FRET pair.

$$E_{13}^{*} = k_{13}/(k_1 + k_{12} + k_{13}), \tag{15}$$

$$E_{23} = k_{23}/(k_2 + k_{23}). \tag{16}$$

When dye 3 bleaches, only FRET interaction between dye 1 and dye 2 exists and their intensities I_1^* and I_2^* can be written as

$$I_1^{*} = 1/(k_1 + k_{12}), \tag{17}$$

$$I_2^{*} = E_{12} \times 1/k_2. \tag{18}$$

In the same way, the intensities of dye 1 and dye 3 when dye 2 bleaches are written as

$$I_1^{\dagger} = 1/(k_1 + k_{13}), \tag{19}$$

$$I_3^{\dagger} = E_{13} \times 1/k_3. \tag{20}$$

Here E_{12} is $k_{12}/(k_1 + k_{12})$ and E_{13} is $k_{13}/(k_1 + k_{13})$. Using E_{12} and E_{13}, k_{12} and k_{13} are expressed

$$k_{12} = E_{12} \times k_1/(1 - E_{12}), \tag{21}$$

$$k_{13} = E_{13} \times k_1/(1 - E_{13}). \tag{22}$$

By inserting Eqs. 21 and 22 into Eqs. 14 and 15, we get E_{12}^* and E_{13}^*,

$$E_{12}^{*} = E_{12} \times (1 - E_{13})/(1 - E_{12} \times E_{13}), \tag{23}$$

$$E_{13}^{*} = E_{13} \times (1 - E_{12})/(1 - E_{12} \times E_{13}). \tag{24}$$

Now, we divide Eq. 12 by Eq. 18, and Eq. 13 by Eq. 20,

$$\begin{aligned} I_2/I_2^{*} &= (E_{12}^{*}/E_{12}) \times [k_2/(k_2 + k_{23})] \\ &= (E_{12}^{*}/E_{12}) \times (1 - E_{23}), \end{aligned} \tag{25}$$

$$I_3/I_3^{\dagger} = (E_{12}^{*} \times E_{23} + E_{13}^{*})/E_{13}. \quad (26)$$

We solve the Eqs. 25 and 26 for E_{23},

$$E_{23} = 1 - I_2/I_2^{*} \times (1 - E_{12} \times E_{13})/(1 - E_{13}), \quad (27)$$

or

$$E_{23} = (I_3/I_3^{\dagger} - (1 - E_{12})/(1 - E_{12} \times E_{13})) \times E_{13} \times (1 - E_{12} \times E_{13})/E_{12}/(1 - E_{13}). \quad (28)$$

I_2/I_2^{*} and $I_3/I_3^{\dagger}$ are readily obtained as 0.72 and 2.71 by comparing relative intensities in regions I, II, and III. As a result, E_{23} is 0.26 from Eq. 27 and 0.36 from Eq. 28. In this conformation, Cy5 is in the high FRET state but Cy5.5 is in the low FRET state and fitting parameters of I_3 and $I_3^{\dagger}$ are more prone to errors. Therefore, by adopting Eq. 27, we get that $D_{23} = 8.7$ nm using $R_0 = 7.3$ nm. In case of the *X*-on-*R* antiparallel state, distances derivation is the same except that energy transfer from Cy5.5 to Cy5 should be included in the interaction map. Distances calculated this way are in general agreement with the expected distances based on the Holliday junction structure (Eichman et al., 2000) and arm lengths (4.8 nm, 8.2 nm, and 7.9 nm for D_{12}, D_{13}, and D_{23} respectively). Yet, we note that the distance estimates made here are only approximate. In calculating R_0 values, we assumed that the orientational factor κ^2 is two-thirds, which is strictly valid only if the fluorophores rotate freely on a timescale faster than the fluorescence lifetime. Fluorescence polarization anisotropy of these dyes attached to the end of duplex DNA ranges from 0.25 and 0.3, and therefore we should consider the calculated R_0 values and experimentally estimated distances as approximate.

CONCLUSION

We have realized the single-molecule three-color FRET technique and measured correlated single-molecule dynamics of DNA Holliday junctions. We anticipate that this technique will be used in detecting complex dynamics of biomolecules and observing binding events between multiple components. Wide-field imaging implementation of three-color FRET will be very useful considering the low yield of molecules with all three fluorophores.

We thank Sean A. McKinney for writing codes for data acquisition programs, Tim Wilson and David Lilley for their providing RNA four-way junctions used for preliminary investigation, and Michelle Nahas for carefully reading the manuscript.

Funding was provided by the National Institutes of Health and the National Science Foundation.

REFERENCES

Clegg, R. M. 1992. Fluorescence resonance energy transfer and nucleic acids. *Methods Enzymol.* 211:353–388.

Duckett, D. R., A. I. Murchie, S. Diekmann, E. von Kitzing, B. Kemper, and D. M. Lilley. 1988. The structure of the Holliday junction, and its resolution. *Cell.* 55:79–89.

Eichman, B. F., J. M. Vargason, B. H. M. Mooers, and P. S. Ho. 2000. The Holliday junction in an inverted repeat DNA sequence: sequence effects on the structure of four-way junctions. *Proc. Natl. Acad. Sci. USA.* 97:3971–3976.

Ha, T., T. Enderle, D. F. Ogletree, D. S. Chemla, P. R. Selvin, and S. Weiss. 1996. Probing the interaction between two single molecules: fluorescence resonance energy transfer between a single donor and a single acceptor. *Proc. Natl. Acad. Sci. USA.* 93:6264–6268.

Ha, T. J., A. Y. Ting, J. Liang, W. B. Caldwell, A. A. Deniz, D. S. Chemla, P. G. Schultz, and S. Weiss. 1999. Single-molecule fluorescence spectroscopy of enzyme conformational dynamics and cleavage mechanism. *Proc. Natl. Acad. Sci. USA.* 96:893–898.

Ha, T. 2001. Single-molecule fluorescence resonance energy transfer. *Methods.* 25:78–86.

Ha, T. 2004. Structural dynamics and procession of nucleic acids revealed by single-molecule spectroscopy. *Biochemistry.* 44:4055–4063.

Haustein, E., J. Michael, and P. Schwille. 2003. Triple FRET: a tool for studying long-range molecular interactions. *Chem. Phys. Chem.* 4:745–748.

Horsey, I., W. S. Furey, J. G. Harrison, M. A. Osborne, and S. Balasubramanian. 2000. Double fluorescence resonance energy transfer to explore multicomponent binding interactions: a case study of DNA mismatches. *Chem. Commun.* 1043–1044.

Joo, C., S. A. McKinney, D. M. J. Lilley, and T. Ha. 2004. Exploring rare conformational species and ionic effects in DNA Holliday junctions using single-molecule spectroscopy. *J. Mol. Biol.* In press.

Lilley, D. M. J. 2000. Structures of helical junctions in nucleic acids. *Q. Rev. Biophys.* 33:109–159.

Liu, J., and Y. Lu. 2002. FRET study of a trifluorophore-labeled DNAzyme. *J. Am. Chem. Soc.* 124:15208–15216.

McKinney, S. A., A.-C. Déclais, D. M. J. Lilley, and T. Ha. 2003. Structural dynamics of individual Holliday junctions. *Nat. Struct. Biol.* 10:93–97.

Murchie, A. I., R. M. Clegg, E. Von Kitzing, D. R. Duckett, S. Diekmann, and D. M. Lilley. 1989. Fluorescence energy transfer shows that four-way DNA junction is a right-handed cross of antiparallel molecules. *Nature.* 341:763–766.

Murphy, M. C., I. Rasnik, W. Cheng, T. M. Lohman, and T. Ha. 2004. Probing single-stranded DNA conformational flexibility using fluorescence spectroscopy. *Biophys. J.* 86:2530–2537.

Nowakowski, J., P. J. Shim, G. S. Prasad, C. D. Stout, and G. F. Joyce. 1999. Crystal structure of an 82-nucleotide RNA-DNA complex formed by the 10–23 DNA enzyme. *Nat. Struct. Biol.* 6:151–156.

Ortiz-Lombardia, M., A. Gonzalez, R. Eritja, J. Aymami, F. Azorin, and M. Coll. 1999. Crystal structure of a DNA Holliday junction. *Nat. Struct. Biol.* 6:913–917.

Ramirez-Carrozzi, V. R., and T. K. Kerppola. 2001. Dynamics of Fos-Jun-NFAT1 complexes. *Proc. Natl. Acad. Sci. USA.* 98:4893–4898.

Selvin, P. R. 2000. The renaissance of fluorescence resonance energy transfer. *Nat. Struct. Biol.* 7:730–734.

Watrob, H. M., C. Pan, and M. D. Barkley. 2003. Two-step FRET as a structural tool. *J. Am. Chem. Soc.* 125:7336–7343.

Weiss, S. 1999. Fluorescence spectroscopy of single biomolecules. *Science.* 283:1676–1683.

Weiss, S. 2000. Measuring conformational dynamics of biomolecules by single molecule fluorescence spectroscopy. *Nat. Struct. Biol.* 7:724–729.